Key Growth Parameters for the Electrodeposition of ZnO Films with an Intense UV−Light Emission at Room Temperature J

ARTICLE *in* THE JOURNAL OF PHYSICAL CHEMISTRY C · JUNE 2009

Impact Factor: 4.77 · DOI: 10.1021/jp9010179

Key Growth Parameters for the Electrodeposition of ZnO Films with an Intense UV-Light Emission at Room Temperature

T. Pauporté,*,† E. Jouanno,† F. Pellé,‡ B. Viana,‡ and P. Aschehoug‡

Laboratoire d'Electrochimie, Chimie des Interfaces et Modélisation pour l'Énergie, UMR 7575 ENSCP-CNRS and Laboratoire de Chimie de la Matière Condensée de Paris, UMR 7574 CNRS-ENSCP-UPMC, École Nationale supérieure de Chimie de Paris, 11 rue P. et M. Curie, 75231 Paris cedex 05, France

Received: February 4, 2009; Revised Manuscript Received: April 7, 2009

The development of efficient low-temperature growth methods for the preparation of high-quality ZnO is a challenge for new generation of optoelectronic devices such as flexible UV-light emitting diodes (LED). We show that the UV emission at room temperature of electrodeposited ZnO is strongly influenced by the growth deposition parameters. The parameters investigated include the bath temperature, the type of anion, the deposition potential, and the oxygen and zinc ion concentrations. It is shown that working at a relatively high bath temperature and at low overvoltage dramatically increases the UV excitonic emission, whereas the visible one due to deep defects becomes negligible. The enhancement is much less marked by working at low oxygen concentration. A more intense UV emission is also observed from ZnO nanorod and nanowire arrays compared to ZnO dense films. The UV emission markedly shifts toward a higher energy when a chloride medium is used. This is assigned to a high n-type doping of ZnO giving rise to a Burstein−Moss effect. The defects possibly at the origin of high carrier concentration are discussed. The present study demonstrates that electrodeposition is a competitive low-temperature growth method for the preparation of UV LED, especially the nanowire-based ones.

1. Introduction

In recent years, ZnO has attracted much attention as a key material for UV-light emitting diodes (LED) and UV-laser diodes.[1] These devices are of utmost interest for a large variety of applications ranging from lighting to lithography processes and large capacity memories.[2,3] ZnO is an intrinsic n-type II−VI semiconductor with a direct dipole allowed band gap of 3.37 eV at room temperature and a large exciton binding energy of ∼60 meV. Because of these properties, ZnO presents a strong excitonic UV-light emission at room temperature. In addition to the excitonic UV-emission, most of ZnO also exhibits a visible emission in the 2.2−2.9 eV range.[4] Its origin has been assigned to various intrinsic defects such as oxygen vacancy (V_O),[1] singly ionized oxygen vacancy ($V^{\bullet}_O$),[5] zinc vacancy (V_{Zn}),[1] interstitial zinc (Zn_i)[6] or oxygen antisite defect (O_{Zn}).[7] As a consequence, the preparation of ZnO for UV emitters must be optimized in order to produce a high-quality material with a minimum intrinsic defect. The emission intensity ratio between the near-band-edge (NBE) excitonic emission and the defect-related visible emission is classically used to evaluate the quality of ZnO crystals.[8]

ZnO can be prepared at much lower temperature than GaN, its main competitor for the above-mentioned applications. Other advantages of ZnO include a high mechanical, chemical, and thermal stability,[9] a high radiation hardness,[10] and biosafety. Among the various growth methods of ZnO, several of them have the special interest of being processed at low temperature. Most often, aqueous solutions are used as the growth medium. Electrodeposition is probably one of the most promising of them.[11−23] The deposition mechanism is based on the generation of hydroxide ions by reduction of a soluble precursor on the conducting substrate which acts as an electrode.[12,23] In the presence of zinc ions in the solution, ZnO is precipitated directly on the electrode surface. When molecular oxygen is used as the precursor,[12,24] the deposition reactions are written as follows:

$$\frac{1}{2}O_2 + H_2O + 2e^- \rightarrow 2\,OH^- \quad (1)$$

$$Zn(II) + 2\,OH^- \rightarrow ZnO + H_2O \quad (2)$$

The method is highly versatile, and one can play on a large variety of growth parameters for controlling the film morphology and properties. Some authors have investigated the PL of electrodeposited ZnO films. Izaki et al. have shown that ZnO films, as-grown on (111)Au/ (100)Si at 65 °C by using a nitrate solution, present mixed NBE excitonic and visible emissions, with a similar intensity.[3] Chen et al.[25] have reported the electrodeposition from nitrate ions and nitric acid solutions of ZnO films that emitted both in the UV and the visible with an UV-to-visible emission ratio higher than 1. The emission efficiencies were promising for applications in optoelectronic devices. Könenkamp et al. have studied ZnO nanorods electrodeposited from a molecular oxygen precursor at 80 °C.[18,19,22] The films presented a rather large amount of defects, and the PL spectrum was dominated by the visible emission. The LED prepared from these films emitted a band in the white-light wavelength region. The low-temperature preparation process was compatible with lightweight plastic substrates, and the same group was able to prepare flexible white LED.[22] Pauporté et al.[14] have observed that the UV luminescence of electrodeposited

* Author for the correspondence, e-mail: thierry-pauporte@enscp.fr.
† Laboratoire d'Electrochimie, Chimie des Interfaces et Modélisation pour l'Énergie.
‡ Laboratoire de Chimie de la Matière Condensée de Paris.

10.1021/jp9010179 CCC: $40.75
Published on Web 05/19/2009

ZnO films was influenced by the anion in the bath with a more intense UV emission when perchlorate was preferred to chloride as the supporting anion. The same group has shown that ZnO nanorods epitaxially electrodeposited on the (0002) plane of a GaN single crystal yielded a stimulated UV emission above an excitation power density threshold of 4.4 $mW.cm^{-2}$.[26]

Low-temperature electrodeposited ZnO has often been described as needing a postannealing treatment in order to enhance dramatically the optical properties and especially the UV excitonic emission. Classically, the thermal annealing is performed at 400−500 °C.[13,19,27] However, a challenge is to avoid additional high-temperature steps and to find deposition conditions for high-quality ZnO synthesis at low temperature. This would pave the way of UV-LED based on low-temperature electrodeposited ZnO with a process compatible with plastic substrates for instance.

The present paper is a systematic study of the main growth parameters of ZnO electrodeposition on the morphological and the optical properties of the oxide. A special attention has been paid on the deposition conditions required to yield high-quality films with an intense UV PL emission and a negligible visible PL emission. We show that, by accurately choosing the growth conditions, dense films and nanorod/nanowire array films of ZnO with an intense UV-light emission at room temperature can be prepared by electrochemical methods.

2. Experimental Section

Electrodeposition was carried out in a three-electrode cell. The counter electrode was a zinc wire, and the reference electrode was a saturated calomel electrode (SCE) (with a potential at +0.25 V vs NHE) placed in a separate compartment maintained at room temperature. The deposits were prepared on F:SnO_2 coated glass substrates (FTO). The substrates were cleaned under ultrasonics, 5 min in acetone, 5 min in ethanol, and 2 min in 45% nitric acid. To ensure a deposition as homogeneous as possible, the substrate was fixed and contacted to a rotating disk electrode (RDE), and the deposition was performed at a constant rotation speed of 300 rotations per minute (rpm). Two deposition media prepared with Milli-Q quality water were investigated. The chloride medium contained 0.2 or 5 mM $ZnCl_2$ and 0.1 M KCl. The perchlorate medium contained 0.2 or 5 mM $Zn(ClO_4)_2$ and 0.1 M $LiClO_4$. The bath was saturated with molecular oxygen, and a slight O_2 bubbling was maintained during the deposition process. The electrochemical cell was placed in a thermostatted bath. The bath temperature was varied between 70 and 88 °C (chosen as the upper limit to avoid solvent evaporation troubles and RDE damages). The temperature was fixed with an uncertainty of ±0.4 °C. The applied potential ranged between −0.6 and −1 V versus SCE. For the films prepared with 5 mM Zn(II), the experiment was stopped when the total electrical charge exchanged, noted Q_{tot}, was 1.1 $C \cdot cm^{-2}$. If one assumes a faradaic efficiency equal to 1, that charge corresponds to a dense film thickness of 820 nm. After deposition, the films were carefully rinsed with Milli-Q water in order to eliminate chloride salts present at their surfaces.

The films were observed with a high-resolution Ultra 55 Zeiss FEG scanning electron microscope. The film thicknesses were measured on cross-sectional views. Energy dispersive X-ray spectroscopy (EDX) analyses were performed with a Bruker silicon drift detector. The diffuse reflectance spectra were measured on a Varian Cary 5E UV−vis-NIR spectrophotometer equipped with an integrating sphere. The optical bandgap of ZnO was calculated from the edge observed on the reflectance spectra, according to the procedure reported in ref 28. Most of the PL measurements were carried out at room temperature and some at 9 K by using a helium cryostat. The excitation source at 266 nm was provided by the YAG:Nd quadrupled frequency. The emission was analyzed by using a HR250 monochromator (Jobin-Yvon) coupled with an UV-enhanced intensified charge coupled device (ICCD, Roper). Under pulsed laser excitation, luminescence spectra were recorded in a pseudo CW mode with a continuous integration of the intensity during 300 ms corresponding to three full illumination pulses. The excitation power and the geometrical arrangement of the experiment were the same for the various investigated samples. All the spectra were normalized by using the emission of the same electrodeposited film as a reference (growth conditions: applied potential −1 V vs SCE, temperature 85 °C, 5 mM $ZnCl_2$ and 0.1 M KCl, Q_{tot}= 1.1 $C.cm^{-2}$). Therefore, the emission intensities in Figures 2, 5, and 8 can be compared. The PL spectra of the films were found to be highly stable in intensity and shape. For instance, the spectrum of the reference sample was unchanged after more than 8 months of storage under ambient conditions.

3. Results and Discussion

3.1. Growth Temperature and Anion Effects. We have previously shown that the deposition temperature is an important growth parameter that governs the crystallinity of ZnO films.[29] The variation of film morphology in the temperature range 70−88 °C for a Zn(II) concentration of 5 mM is shown in Figure 1. Two different media have been investigated, a chloride medium and a perchlorate medium. The films are made of crystallites that are more or less merged, and it has been shown elsewhere that each crystallite is a single crystal.[16] We observe that for both anions, the temperature increase leads to the formation of crystallites with a smaller width (Table 1). The films prepared at 70 °C in chloride medium (Figure 1a) and perchlorate medium (Figure 1d) are dense and rather smooth in the case of chloride medium. At higher deposition temperature, the rods are merged at their bottom and separated at their top. The structures are more open at higher temperature with a higher film thickness in the chloride medium (Table 1). The density increases from 10 crystallites μm^{-2} at 70 °C up to 15−16 crystallites μm^{-2} at 88 °C. Increasing the temperature results in a higher initial density of nuclei and in a decrease in the lateral growth rate of the crystallites. The grain surface aspect depends on the anion with smoother surfaces in the case of chloride medium. The crystallites present well-faceted hexagonal shape at 70 °C. In perchlorate medium, the grains have a rough surface, especially at 70 °C.

The mean current density, noted j_m, is reported in Table 1 for the various growth conditions. This parameter decreases with the temperature, and the oxygen reduction reaction is not activated at higher bath temperature. j_m is also significantly smaller in the case of chloride medium compared to perchlorate medium. This suggests an adsorption phenomenon of the anion that impedes the reduction rate of molecular oxygen and then the growth of ZnO. This observation is in agreement with recent results on the significant decrease in the molecular oxygen reduction rate with increasing chloride ion concentration upon the growth of ZnO nanowires.[20] Much less interactions are found in the case of perchlorate anions because the deposition current density is significantly higher.

The nature of the anion in the growth medium affects the chloride content of the deposited film. In Table 1 is reported the ratio between chlorine atomic % and zinc atomic % measured by the EDX technique. Cl content was measured from

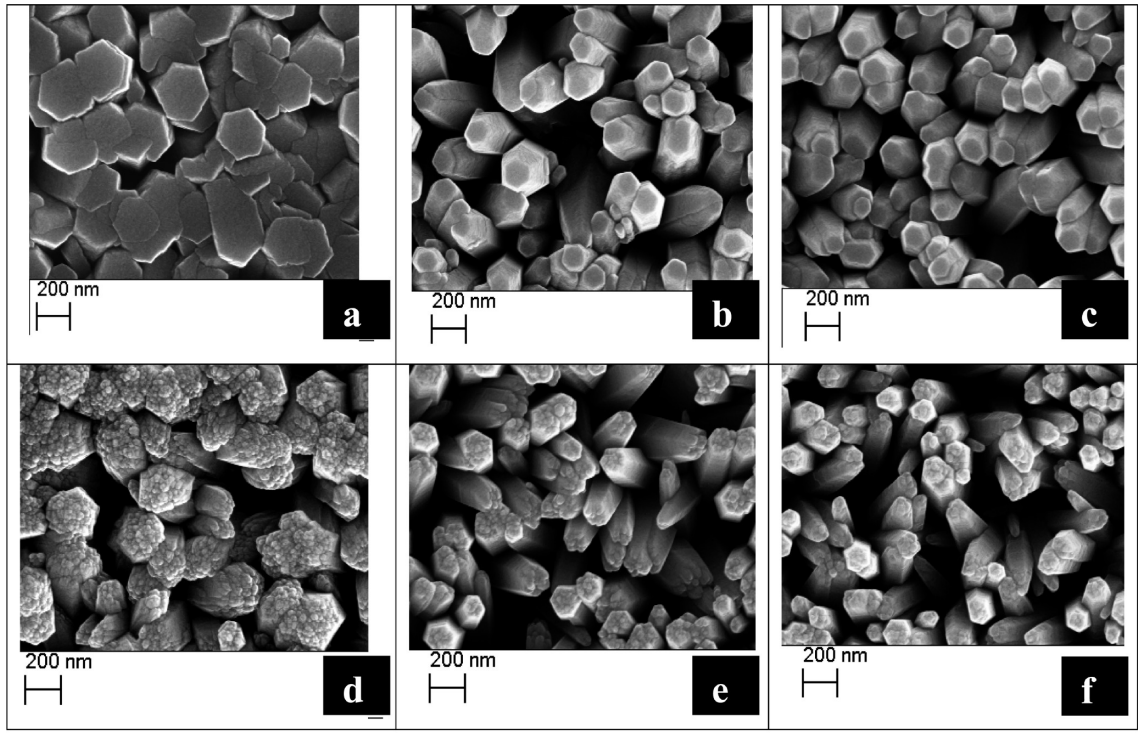

Figure 1. Effect of deposition temperature SEM top views of films prepared with [Zn(II)] = 5 mM, −1 V/SCE, in chloride (a,b,c) and perchlorate (d,e,f) media at 70 °C (a,d), 85 °C (b, e), and 88 °C (c,f).

TABLE 1: Effects of Deposition Temperature and Supporting Anion on the Morphology, Optical Properties, and Composition of ZnO Films ([Zn(II)] = 5 mM, Q_{tot} = 1.1 C.cm^{-2}, E_{appl}= −1 V/ SCE)

	medium					
	Cl^-			ClO_4^-		
temperature	70 °C	85 °C	88 °C	70 °C	85 °C	88 °C
j_m[a] /mA·cm^{-2}	−0.64	−0.56	−0.58	−0.8	−0.75	−0.71
film thickness /μm[b]	0.85	1.0	1.1	1.0	1.1	1.0
crystallite width /nm	400	250	250	400	150	100
crystallite density /μm^{-2}	10	14	15	10	16	16
E_{exc} /eV[c]	3.44	3.32	3.32	3.30	3.23	3.25
E_g /eV[d]	3.46	3.37	3.38	3.27	3.25	3.27
I_{UV}/I_{vis}[e]	1.3	13	39	1.5	16	37
Cl content /%[f]	3.3−4.0	2.2	2.2	0.38	0.19	0.17

[a] Mean current density. [b] Measured from cross-sectional SEM views. [c] Energy of the excitonic UV photoemission. [d] Optical bandgap calculated from the diffuse reflectance spectra. [e] Intensity ratio between the maxima of the UV emission and of the visible emission. [f] Defined as Cl at.% /Zn at.% measured by EDX.

the intensity of the K signal at 2.63 keV and Zn content from the intensity of the K signal at 8.61 keV. The intensity ratio between the L line and the K line of Zn was similar to that of a flat Zn reference sample showing no significant disturbance due to roughness on the EDX measurements of our samples. At 70 °C, a large amount of chlorine was incorporated in the film (3.3−4.0%), whereas at higher temperatures, the quantity was divided by about 1.5−2. The incorporation of chlorine in the film can be understood from the complexing properties of Cl^- for Zn^{2+}. One of the author has shown that above 50 °C, in the present bath conditions, Zn^{2+} is complexed by chloride ions, and the dominant Zn(II) species is $ZnCl^+$.[29] $ZnCl^+$ represents 65% of Zn(II) in solution at 70 °C and 82% at 90 °C. Much less concentration of chlorine is detected in the deposited films. Most part of chloride ions are released in the solution during the ZnO molecular unit formation and film growth. A small fraction of them is entrapped in the ZnO. The film chlorine content decreases significantly with the deposition temperature, and then, chloride release is favored at high temperature (Table 1). A smaller quantity of chlorine is contained in the film prepared in perchlorate medium (Table 1). This is likely due to the poor complexing properties of ClO_4^- for Zn^{2+}. This anion is also more difficult to incorporate in ZnO because of a larger size. It is worth noting that chlorine content in films grown at high temperature in this medium is negligible.

The optical properties of the films were investigated by PL and diffuse reflectance measurements. Figure 2A shows that the diffuse reflectance (R) spectra present a maximum at 400 nm, preceded by a sharp edge in the UV-wavelength range due to the semiconducting properties of ZnO. In the visible-wavelength range, R is promoted at 85−88 °C because of a higher surface roughness and light scattering. PL characterizations have been used to probe the presence of native defects in the films and, then, their structural and optical quality. They also give information on the potential brightness of the material for an application in light-emitting devices. Figure 2B,C shows that the PL spectra of electrodeposited ZnO film are highly influenced by the growth temperature. At 70 °C, the films

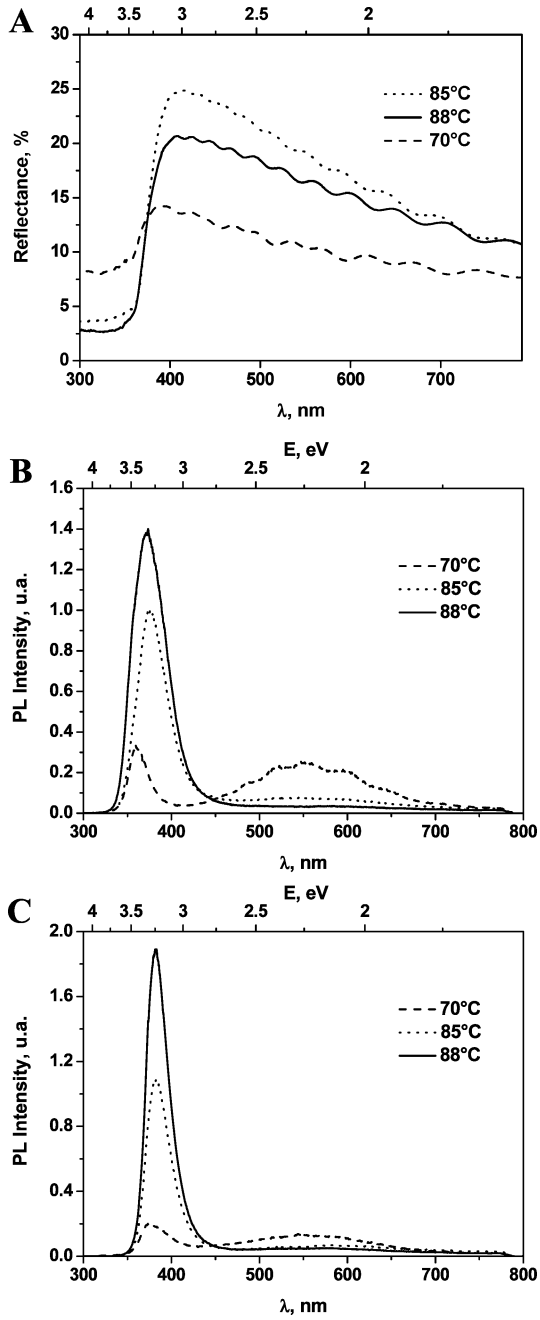

Figure 2. (A,B) ZnO films prepared in 5 mM $ZnCl_2$ + 0.1 M KCl at various temperatures and at $E_{appl} = -1$ V/SCE. (A) Diffuse reflectance spectra. (B) Normalized PL spectra. (C) Normalized PL spectra of films prepared from 5 mM $Zn(ClO_4)_2$ + 0.1 M $LiClO_4$.

present two emission peaks of low intensity: a NBE emission in the UV and a green emission centered at 2.25 eV due to deep defects (V_O, $V^{\bullet}_O$, etc). The intensity ratio between the maximum of the two emissions is a good fingerprint of the quality of the material.[3,8] At this temperature, the I_{UV}/I_{vis} intensity ratio is above 1 but not high (Table 1). Figure 2B,C demonstrates that the deposition temperature is a key parameter to grow high-quality ZnO because the UV NBE emission is dramatically promoted by increasing the temperature, whereas the visible one is markedly depleted. The lower density of intrinsic defects at higher temperature can be assigned to a slower growth rate and a higher surface mobility of the species. We can also suppose that the presence of a large amount of chlorine in the film promotes the formation of defects that favor the nonradiative deexcitation of the excitons and the visible emission. At

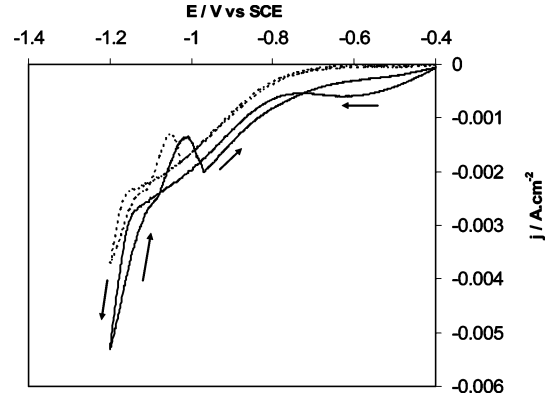

Figure 3. Cyclic voltammetry at 88 °C of electrodeposited ZnO disk electrode in a 5 mM $ZnCl_2$ + 0.1 M KCl solution (dashed line) and in a 5 mM $Zn(ClO_4)_2$ + 0.1 M $LiClO_4$ solution (full line). Solution saturated with O_2.

88 °C, the film prepared in perchlorate presents a narrower and more intense UV peak compared to the film prepared in chloride medium.

The wavelength of the UV emission is another important parameter of the ZnO PL emission. Depending on the electrodeposition conditions, it can vary between 3.23 and 3.44 eV (Table 1). Therefore, it is possible to control the wavelength of the emission within a 0.21 eV range by simply changing the growth conditions. Similar variations have been reported by Pauporté et al. for the bandgap energy of electrodeposited ZnO.[14] The high excitonic emission energy observed at low growth temperature in chloride medium (3.44 eV) is surprising but in good agreement with the high optical bandgap energy measured on these samples by reflectance spectroscopy (3.46 eV, Table 1). Several hypotheses can be put forward to explain the enlargement of the bandgap energy of ZnO. One can invoke the presence of small fraction of hydroxide or strain in the film.[14] However, recent results have shown that ZnO prepared electrochemically in chloride medium has a high charge-carrier concentration.[30] Therefore, another possibility is a bandgap widening due to a high n-type doping of ZnO samples. In that case, the bottom of the conduction band is filled and blocked. The phenomenon is known as band filling effect or Burstein−Moss (BM) effect.[31−33] We can point out that a carrier concentration ranging between 2×10^{19} and 10^{20} cm^{-3} is sufficient to observe the BM effect in zinc oxide.[32] Such values can be attained at low intrinsic or extrinsic dopant concentration with values of ∼0.03−0.13% for single electron donors (defined as [dopant]/[Zn]+[O]). Consequently, it is a rather difficult task to determine the defect at the origin of the PL UV-emission energy enlargement.

Some authors have suggested the role of Zn_i because of the drop in carrier concentration after sample annealing.[34] Doping by oxygen vacancies, V_O, can also be considered here because of the green PL emission of the highly doped samples. On the other hand, several papers have considered recently the use of chlorine for the n-doping of ZnO.[35−39,30] Oxygen atoms can be substituted by chlorine atoms in the ZnO crystallographic lattice, in which they act as donors.[37] Doping by oxygen vacancies (V_O) appears as very unlikely because it has been observed by XRD that the lattice parameters are enlarged for the highly doped samples (results not shown). An expansion of the ZnO lattice parameter is expected from either Zn_i-doping[33] or Cl-doping.[37] Replacing O by Cl gives rise to a larger Zn−Cl interatomic distance (2.38−2.43 Å) compared to the Zn−O distance (1.97 Å).[37] However, doping by Zn_i can be ruled out because the PL

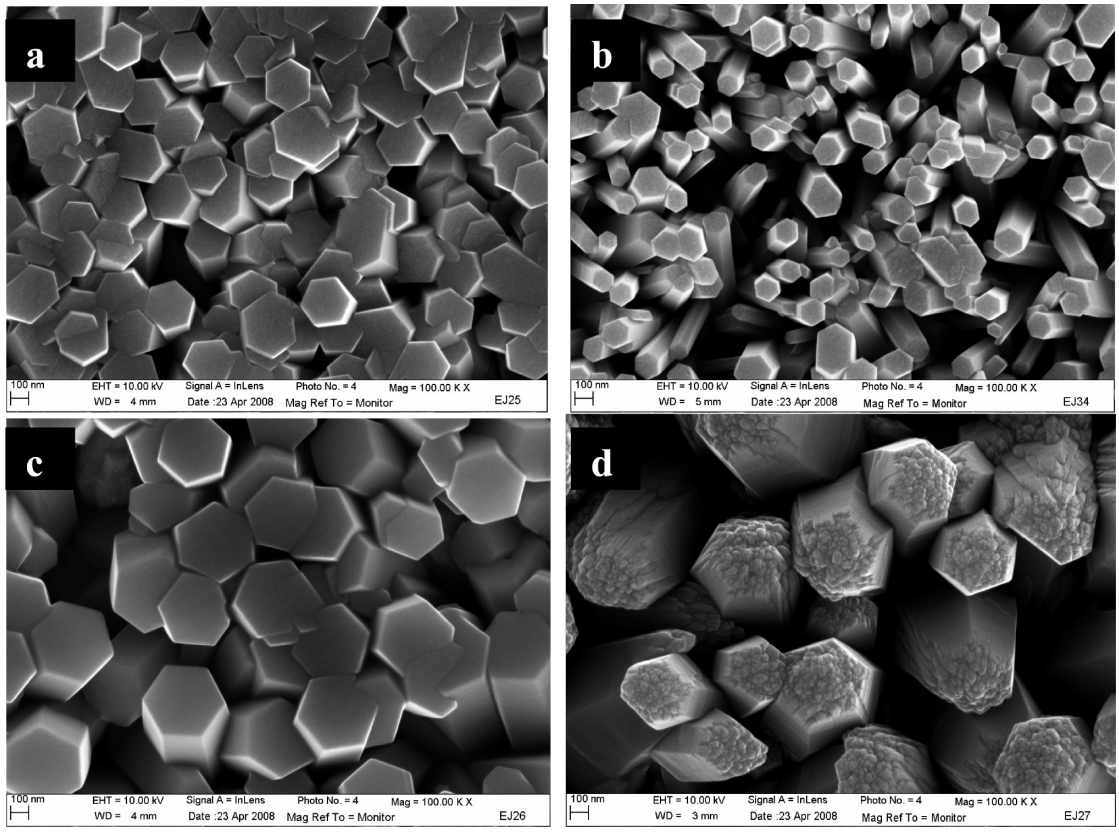

Figure 4. SEM top views of electrodeposited ZnO films, $Q_{tot} = 1.1$ C.cm^{-2}. (a,b) Effect of deposition potential. (a) 5 mM $ZnCl_2$ + 0.1 M KCl, 88 °C, −0.78 V/SCE, solution saturated with oxygen (0.8 mM). (b) 5 mM $Zn(ClO_4)_2$ + 0.1 M $LiClO_4$, 88 °C, −0.60 V/SCE, $[O_2] = 0.8$ mM. (c,d) Effect of oxygen concentration. (c) 5 mM $ZnCl_2$ + 0.1 M KCl, 70 °C, −1 V/SCE, $[O_2] = 0.2$ mM. (d) 5 mM $Zn(ClO_4)_2$ + 0.1 M $LiClO_4$, 70 °C, −1 V/SCE, $[O_2] = 0.2$ mM.

spectra of the samples do not exhibit the violet PL emission characteristic of Zn_i at about 2.9 eV.[39] If we consider now the doping by Cl, it could seem compatible with EDX titrations of our samples (Table 1) because we observe an enlarged bandgap for the Cl-rich samples. Chlorine content in the films is much higher than that necessary for doping. However, the doping by chlorine is also debatable in view of results on sample annealing. After heating a Cl-rich sample at 400 °C during 1 h, Cl content is decreased by only ∼20%, whereas the bandgap energy drops to the classical value of 3.28 eV, and the excitonic UV emission energy is 3.24 eV.[40]

The origin of high donor concentration in samples as-grown in chloride medium remains an open question, and further investigations are needed to give a definitive answer. It cannot be excluded that the presence of Cl^- in the bath favors the incorporation of some intrinsic defects which remain to be clearly identified.

3.2. Effects of Deposition Potential. The electrochemical potential used for the deposition is expected to influence the quality of the ZnO films because this parameter controls notably the current density and then the growth rate of the layer. To determine the potential window for ZnO electrodeposition, cyclic voltammograms (CV) have been recorded on dense ZnO layers (Figure 3). Two media have been investigated, a chloride medium and a perchlorate medium. For the former study, a thin ZnO prelayer was deposited in 5 mM $ZnCl_2$ + 0.1 M KCl at 70 °C during 10 min. For the latter study, the prelayer was deposited in 5 mM $Zn(ClO_4)_2$ + 0.1 M $LiClO_4$ at 70 °C for 10 min. During CV, the electrode was rotated at 300 rpm. Higher current densities were recorded in perchlorate medium in good agreement with the discussion in the previous section. The positive deposition boundary is limited by the oxygen reduction wave, whereas the negative one is limited by the reduction of Zn(II) into metallic zinc.[12] A consequence is that the ZnO deposition window ranges between −0.78 and −1.1 V in chloride medium and between −0.6 and −1.1 V in perchlorate medium. Because of a very low current density, no deposit was observed above −0.6 and −0.78 V in perchlorate and chloride medium, respectively. In the CV, the reoxidation of metallic zinc into Zn(II) can be seen when the scan direction is reversed with a peak centered at about −1 V.

Figures 1c,f and 4a,b and Table 2 summarize the influence of the deposition potential on the film morphology. In both chloride and perchlorate media, the grain density, size, and length are unchanged at higher potential (Table 2). Comparisons of Figures 1c and 4a for chloride as well as Figures 1f and 4b for perchlorate show that a low overvoltage favors the formation of crystallites with well-defined facets and that a low growth rate promotes the formation of grains with a regular hexagonal shape. The PL spectra of the films are presented in Figure 5A,B. The UV-NBE emission is dramatically enhanced at higher deposition potential (low overpotential), whereas the deep defect emission in the visible becomes negligible. The visible emission is absent for the films grown in chloride medium, and the I_{UV}/I_{vis} intensity ratio is about 68 for the best film grown in perchlorate medium (Table 2). The film quality is promoted because of a slow growth rate which avoids the defect formation in the deposited material.

3.3. Effects of Molecular Oxygen Concentration. Concentration of molecular oxygen is another important parameter for the control of the current density and consequently of the growth rate of the films. Figure 6 shows the effect of molecular oxygen

TABLE 2: Effects of Deposition Potential and Supporting Anion on the Morphology and Optical Properties of ZnO Films ([Zn(II)] = 5 mM, T=88°C, Q_{tot} = 1.1 C.cm^{-2})

	medium						
	Cl^-			ClO_4^-			
E_{appl} /V vs SCE	−0.78	−0.80	−1.00	−0.60	−0.76	−0.80	−1.00
j_m /mA·cm^{-2}	−0.07	−0.08	−0.58	−0.13	−0.20	−0.32	−0.71
film thickness /μm	1.1		1.1	1.0	1.3	1.1	1.0
crystallite width /nm	300		250	150	100−250	150	100
crystallite density /μm^{-2}	15		15	20	6	10	16
E_{exc} /eV	3.32	3.32	3.32	3.23	3.22	3.25	3.25
E_g /eV	3.36	3.38	3.38	3.25	3.24	3.24	3.27
I_{UV}/I_{vis}	>200	>200	39	68	55	40	37

TABLE 3: Effects of Molecular Oxygen Concentration and Supporting Anion on the Morphology and Optical Properties of ZnO Films ([Zn(II)] = 5 mM, E_{appl} =−1 V /SCE, Q_{tot} = 1.1 C.cm^{-2}, T=70°C)

	medium					
	Cl^-			ClO_4^-		
[O2] /mM	0.2	0.4	0.8	0.2	0.4	0.8
j_m /mA·cm^{-2}	0.19	0.38	0.64	0.28	0.45	0.8
thickness /μm	0.9	0.9	1.2	1.4	1.1	1.0
crystallite width /nm	400−500	300−400	300−400	400−600	300−500	200−300
crystallite density /μm^{-2}	5	9	10	2	4	10
E_{exc} /eV	3.36	3.38	3.44	3.26	3.25	3.30
E_g /eV	3.36	3.42	3.45	3.29	3.29	3.27
I_{UV}/I_{vis}	1.3	4.5	25.2	1.5	2.7	9.8

TABLE 4: Comparison of the Growth Rate and PL Properties at Room Temperature of Dense ZnO Films and Nanorod Array Films (E=−1 V/ SCE)

	Cl^-			ClO_4^-		
[Zn(II)] /mM	5	0.2		5	0.2	
temperature / °C	70	85		70	85	
length /μm	0.85	1.1	1.6	1.0	0.75	1.1
Q_{tot} /C·cm^{-2}	1.1	4.9	6.5	1.1	6.8	7
growth rate /μm·h^{-1}	1.9	0.7	1.2	2.6	0.4	0.8
E_{exc}	3.44	3.23	3.23	3.27	3.23	3.23
I_{UV}/I_{vis}	1.3	11	35	1.5	2.8	10

concentration on chronoamperograms of films grown at 70 °C. The electrode was rotated at 300 rpm, and the experiment was stopped after a total electrical charge exchange of 1.1 C.cm^{-2}. Under these conditions, the saturation molecular oxygen concentration is 0.8 mM,[29] whereas lower concentrations were achieved by mixing O_2 with argon at a controlled flow rate. The shape of the chronoamperograms depends on the molecular oxygen concentration. It can be explained by the nucleation−growth and grain-merging processes.[14] The mean current density depends on the molecular oxygen concentration and is not proportional to this parameter, probably because of different roughness of the samples prepared at various precursor concentrations. Figures 1a and 4c compare the morphology of the film at high and low oxygen concentration in chloride medium, and Figures 1d and 4d provide a comparison for the perchlorate medium. One can observe that the density of rods is dramatically decreased at lower precursor concentration and that the mean rod width is increased (Table 3). The first parameter can be explained by a lower sursaturation at the nucleation step, giving rise to a lower nuclei density. The lower rod density favors the lateral growth of the crystallites.

Figure 5C,D shows the effect of the oxygen concentration on the PL properties of the films. At the lowest oxygen concentration, the visible emission is quenched, whereas the UV-NBE emission is promoted. Better properties are obtained in chloride medium compared to perchlorate. The better structural properties at low O_2 concentration can be linked to a lower growth rate and then to a lower incorporation of defects. However, for the same deposition current density, the UV emission is much higher at low overvoltage than at low oxygen concentration.

3.4. Effects of the Nanostructure. Electrodeposition has emerged recently as an interesting technique to grow a large variety of nanostructures. The preparation of ZnO nanorod and nanowire arrays has attracted much attention with the aim of elaborating new generation of devices such as lasers,[2,26] LED,[19,41] solar cells,[42,43] gas sensors,[44] field emission[45,46] or piezoelectric devices,[47] and superhydrophobic surfaces.[48] ZnO wires are formed upon electrodeposition by working at low Zn(II) concentration in the bath because of the blocking of the lateral growth at an early stage.[26] Figure 7 shows wires prepared at 85 °C from chloride and perchlorate solutions containing 0.2 mM Zn(II). The former presents a high aspect ratio of 15 and above. The wires grown in perchlorate medium have a sharp conical edge that may be interesting for field-emission applications.[49] Figure 8 compare the PL properties of dense films and that of ZnO-nanowire array films prepared at 70 °C. It is observed that, in both deposition media, the UV luminescence is dramatically promoted in the ZnO nanowires compared to that in the dense films in spite of a smaller amount of deposited material in the case of the wires. The higher I_{UV}/I_{vis} ratio confirms the better quality of the wires. Comparison of panels A and B in Figure 8 shows that the effect of the anion is opposite to that observed in the case of dense films: the UV emission is significantly more

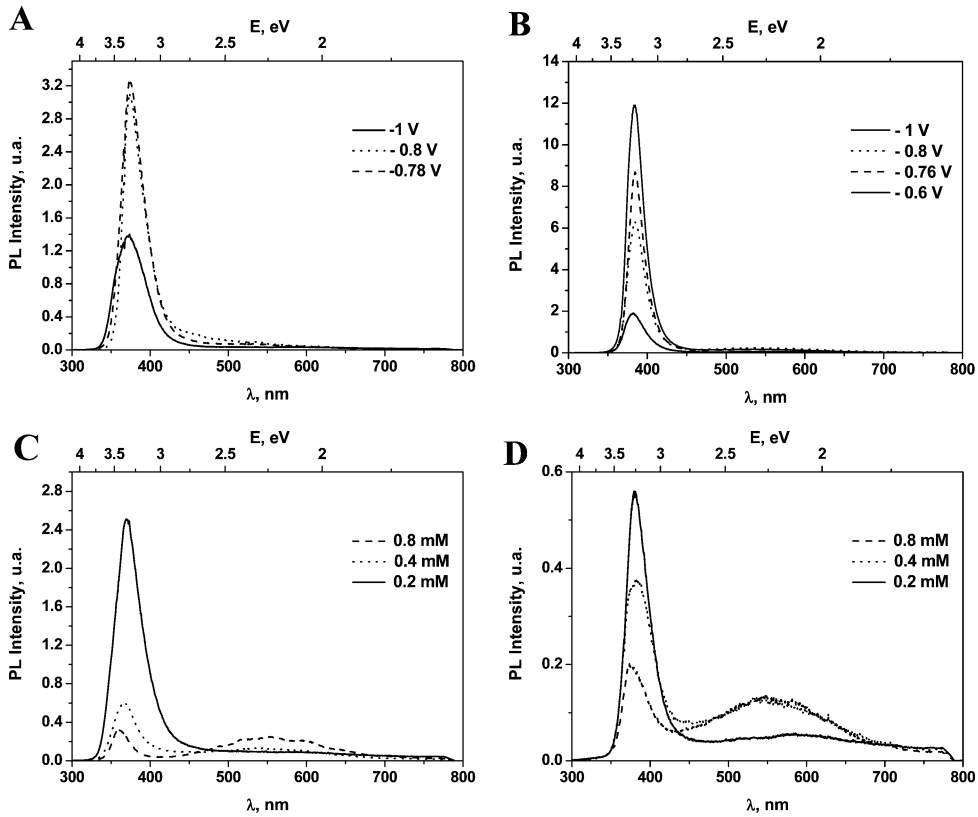

Figure 5. PL spectra of electrodeposited ZnO films, $Q_{tot} = 1.1$ C.cm^{-2}. (A,B) Effect of the deposition potential ($T = 88$ °C). (A) Chloride medium. (B) Perchlorate medium. (C,D) Effect of molecular oxygen concentration ($T = 70$ °C). (C) Chloride medium. (D) Perchlorate medium.

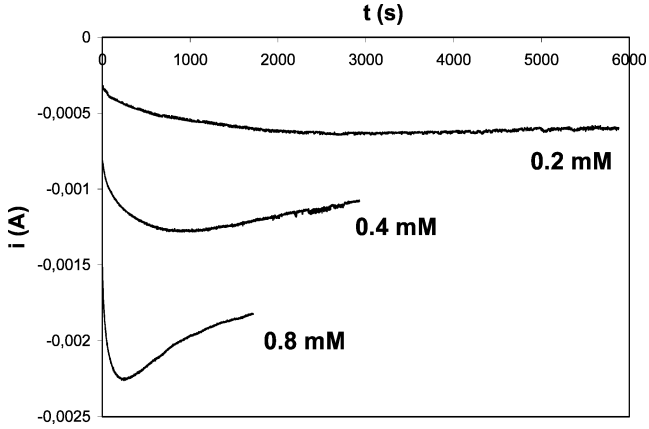

Figure 6. Effect of [O_2] on the chronoamperogramms during ZnO thin film depositions in a 5 mM $ZnCl_2$ + 0.1 M KCl solution at 70 °C (surface area = 3.14 cm^2).

intense in the case of the chloride medium compared to perchlorate medium. The weak visible emission confirms the good quality of the wires. The better quality of the nanowires compared to the dense film for similar growth conditions is likely due to a slower growth rate along the *c*-axis. The growth rate decreases from 1.9 μm·h^{-1} (dense film) down to 0.7 μm·h^{-1} (nanowires) in the chloride medium and from 2.6 μm·h^{-1} down to 0.4 μm·h^{-1} in the perchlorate medium. The reason for the better quality of the nanowires grown in chloride medium remains unclear. The nanowire growth regime is characterized by a low faradaic efficiency compared to dense films, and the charge exchanged is drastically higher for the growth of films in the micrometer range (Table 4). Another interesting feature of the wires prepared in chloride medium compared to the dense films is a significant lower energy for the UV emission (Table 4). The energy is high for the dense film (3.44 eV) and more classical for the rods (3.23 eV). This is in agreement with the stimulated emission at 381 nm that we have reported recently for epitaxial electrochemical nanorods.[26]

Figure 8 also compares the PL emission of rods deposited at 70 and 85 °C. The UV emission intensity and the I_{UV}/I_{vis} emission ratio are markedly increased with the deposition temperature (Table 4). The growth rate remains low compared to dense films, and the better quality can be assigned to the higher mobility of the precursors on the crystal surface giving rise to a lower probability to produce a defect site.

5. Optimization of the Excitonic UV Emission. The above study has highlighted that, for dense films, the best UV emission in chloride medium is obtained for a deposition potential between −0.78 and −0.8 V, a temperature of 88 °C, and a Zn(II) concentration of 5 mM (sample A). In perchlorate medium, the best film was synthesized at a potential of −0.6 V versus SCE, a high temperature of 88 °C, and a Zn(II) concentration of 5 mM (sample B). To better understand the origin of the UV emission of the best samples, temperature-dependent PL measurements were performed. At 300 K, the UV emission can be decomposed into two components (Figure 9a). They are assigned to free exciton (FX) and one-longitudinal-optical phonon replica of the free excitons (FX-1LO) that usually dominate the phonon-assisted emission process at room temperature.[50] At 9 K, the spectra do not present fine structures (Figure 9b). However, the shape of the emission peak can be understood by assuming four different contributions: FX, donor bound excitons (DX), and phonon-assisted FX emissions (FX-1LO and FX-2LO). A satisfactory fit is found for both samples. The fit shows that the low-temperature UV emission of sample A is dominated by the FX emission and that of sample B by DX emission. The emission energies of FX, DX, FX-1LO, and FX-2LO are found

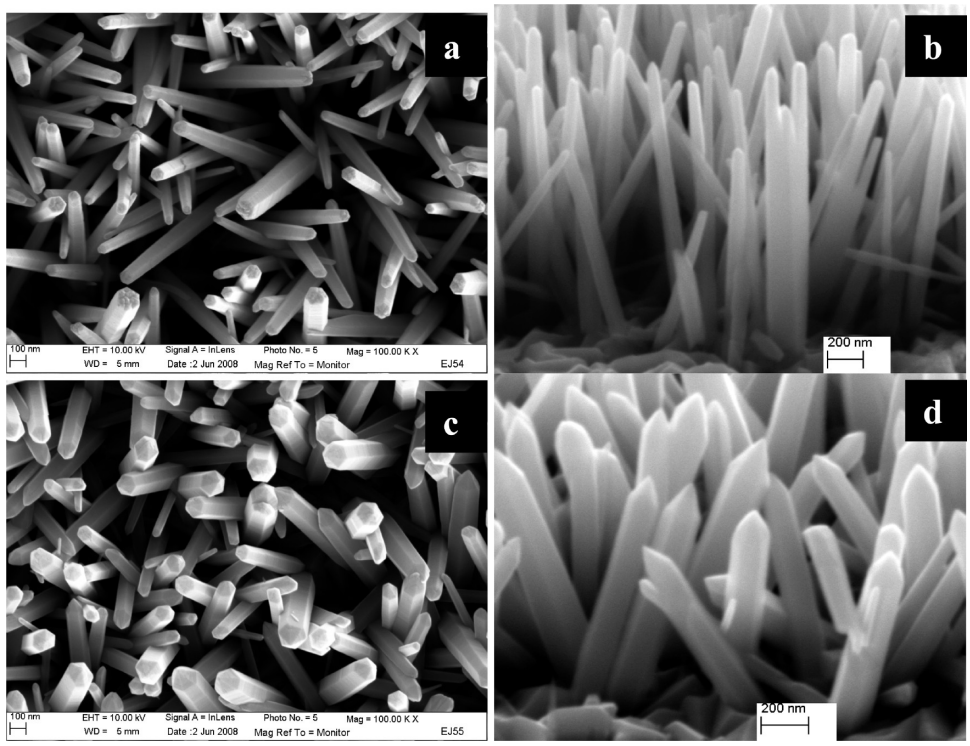

Figure 7. Effect of the nanostructure: SEM views of high quality ZnO nanorod array films prepared at 85 °C, $E_{appl} = -1$ V /SCE, $[O_2] = 0.8$ mM. (a,c) top views; (b,d) tilted views. (a, b) 0.2 mM $ZnCl_2$ + 0.1 M KCl, $Q_{tot} = 6.5$ C.cm^{-2}, $t_d = 5400$s. (c, d) 0.2 mM $Zn(ClO_4)_2$ + 0.1 M $LiClO_4$, $Q_{tot} = 7.0$ C.cm^{-2}, $t_d = 5400$s.

at 3.388, 3.365, 3.313, and 3.218 eV, respectively, for sample A and at 3.353, 3.335, 3.295, and 3.214 eV, respectively, for sample B. The phonon energy deduced from the separation of FX and FX-1LO peaks are 75 meV for sample A, and the average value is 69 meV for sample B. They are in rather good agreement with the value at the absolute temperature of LO phonon in ZnO (71−73 meV).[1]

The temperature dependence of the UV emission energy of samples A and B is presented in Figure 9c. The emission energy decreases with the temperature. The temperature dependence of sample B is dominated by the transition between a DX emission at low temperature and the FX emission at room temperature. In the case of sample A, the emission is dominated by the FX emission over the whole temperature range. The temperature dependence of energy position of the FX-related emission in semiconductor material can be described by the Varshni equation:[51]

$$E(T) = E(0) - \alpha T^2/(T + \beta)$$

where $E(0)$ is the free exciton energy of ZnO at the absolute temperature and α and β are the Varshni thermal coefficients. The solid line in Figure 9c shows that the experimental points are well fitted by the equation, and the parameters found are $E(0) = 3.378$ eV, $\alpha = 4.9\ 10^{-4}$ eV/K, and $\beta = 482$ K.

The present work has highlighted the key role of the deposition current density on the control of the quality of electrodeposited ZnO. The current density can be monitored by changing the applied potential, the deposition temperature, and also the molecular oxygen concentration. In deposition baths presenting an excess of Zn(II), the current density is related to the growth rate of ZnO because most of the electrogenerated OH^- react with Zn(II) to form ZnO molecular units. Figure 10a shows that the energy of the UV excitonic emission is dependent

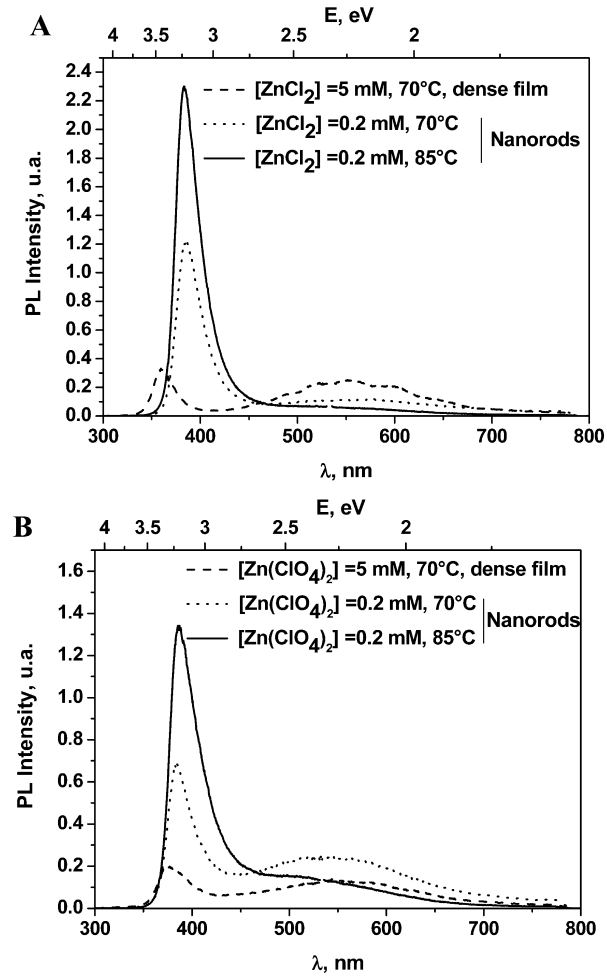

Figure 8. Effect of film structure on room temperature PL emission. (A) Chloride medium. (B) Perchlorate medium.

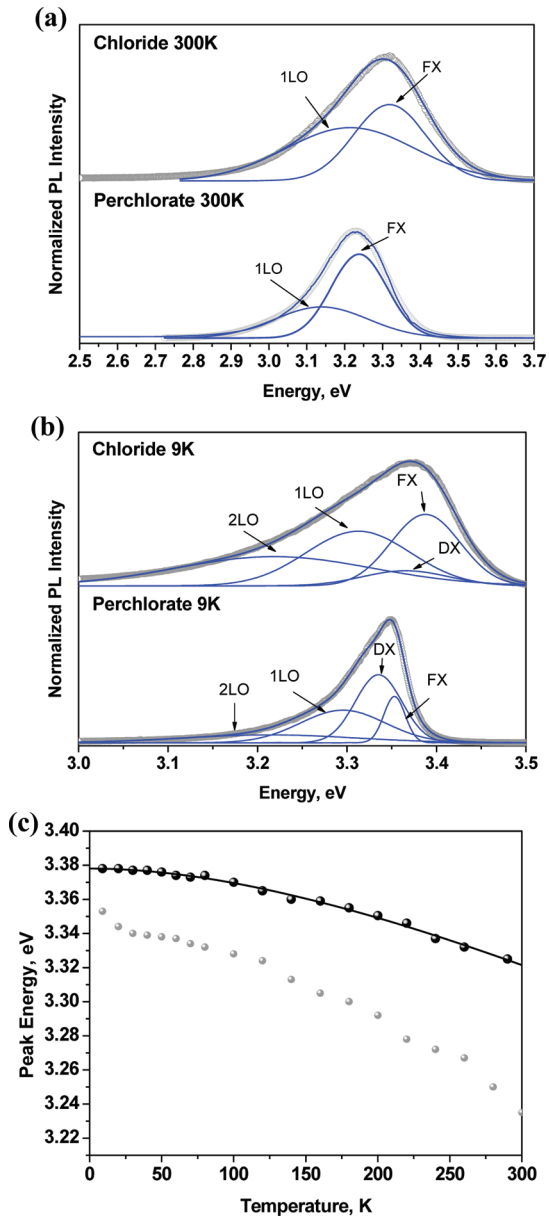

Figure 9. (a,b) Band-edge emission of sample A (chloride) and B (perchlorate); see text for the growth conditions. The open circles are the measured points, and the full lines are the fits. (a) Measurement at 300 K. (b) Measurement at 9 K. (c) Temperature-dependent UV-emission peak position of samples A and B. Black dots, experimental sample A; gray dots, experimental sample B; full line, fit obtained by using the Varshni equation (see text).

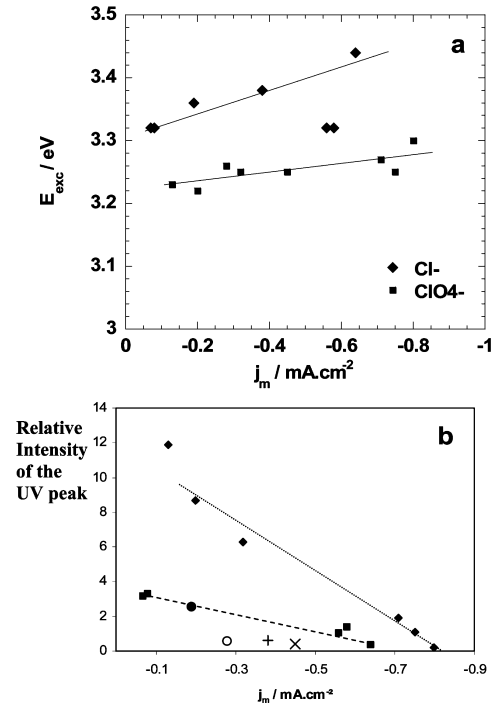

Figure 10. (a) Energy of the excitonic UV emission at room temperature of dense ZnO films grown in perchlorate and in chloride media as a function of j_m. j_m was varied by changing the growth temperature, the applied potential, and the molecular oxygen concentration. (b) Relative intensity of the UV emission of the dense ZnO films prepared by electrodeposition under various conditions as a function of the mean cathodic current density. The emission intensity of the reference is fixed at 1. Chloride medium, $[O_2] = 0.8$ mM (■), $[O_2] = 0.4$ mM (+), $[O_2] = 0.2$ mM (●); Perchlorate medium, $[O_2] = 0.8$ mM (♦), $[O_2] = 0.4$ mM (X), $[O_2] = 0.2$ mM (○). At 0.8 mM, j_m was varied by playing on the deposition temperature and the applied potential.

on the deposition medium and also on the cathodic current density. It is higher in chloride due to the BM effect, and it also increases with the current density because high deposition rate promotes defect entrapment and n-type doping. The variation of the relative UV excitonic emission as the function of the mean current density presents a more complex behavior (Figure 10b). Globally, increasing the deposition temperature or the applied potential increases rapidly the UV emission. For a given medium, the points are included in a similar trend curve. The values for perchlorate medium are located above those for the chloride medium. The films prepared in the former are of much better quality than those prepared in the latter. Significantly lower quality improvement is found by decreasing the oxygen-concentration parameter. The experimental points are located below the two tendency straight lines presented in Figure 10b. The effect is particularly pronounced in the case of the perchlorate medium. The films prepared at low oxygen concentration are poorly luminescent in the UV.

4. Conclusions

The photoluminescence properties of electrodeposited ZnO are dramatically influenced by the deposition parameters. We have observed that working at a relatively high bath temperature and at low overvoltage drastically increases the UV excitonic emission, whereas the visible one due to deep defects becomes negligible. The enhancement is much less marked by working at low oxygen concentration. A more intense UV emission is also found for ZnO nanorod/nanowire arrays compared to ZnO dense films. The UV-emission energy markedly shifts toward higher values when a chloride medium is used. This is assigned to a high carrier concentration in ZnO. The layers can exhibit a strong n-type doping by the method. The study clearly demonstrates that electrodeposition is a competitive low-temperature method for the growth of high quality ZnO.

Acknowledgment. The work was partially funded by a C-nano Ile-de-France program (Project nanoZnO-LED).

References and Notes

(1) Özgür, Ü.; Alivov, Y. I.; Liu, C.; Teke, A.; Reshchikov, M. A.; Dogan, M. A.; Avrutin, V.; Cho, S. J.; Morkoc, H. *J. Appl. Phys.* **2005**, *98*, 041301.

(2) Huang, M. H.; Mao, S.; Feick, H.; Yan, H.; Wu, Y.; Kind, H.; Weber, E.; Russo, R.; Yang, P. *Science* **2001**, *292*, 1897.

(3) Izaki, M.; Watase, S.; Takahashi, H. *Adv. Mater.* **2003**, *15*, 2000.
(4) Ahn, C. H.; Kim, Y. Y.; Kim, D. C.; Mohanta, S. K.; Cho, H. K. *J. Appl. Phys.* **2009**, *105*, 013502.
(5) Vanhauheusden, K.; Warren, W. L.; Seager, C. H.; Talland, D. R.; Voigt, J. A.; Gnade, B. E. *J. Appl. Phys.* **1996**, *79*, 7983.
(6) Bylander, E. G. *J. Appl. Phys.* **1978**, *49*, 1188.
(7) Lin, B.; Fu, Z.; Jia, Y. *Appl. Phys. Lett.* **2001**, *79*, 943.
(8) Chen, Y.; Bagnall, D. M.; Koh, H. J.; Park, K. T.; Hiraga, K.; Zhu, Z.; Yao, T. *J. Appl. Phys.* **1998**, *84*, 3912.
(9) Park, W. I.; Jun, Y. H.; Jung, S. W.; Yi, G. C. *Appl. Phys. Lett.* **2003**, *82*, 964.
(10) Burlacu, A.; Ursaki, V. V.; Skuratov, V. A.; Lincot, D.; Pauporté, T.; Elbelghiti, H.; Rusu, E.; Tiginyanu, I. M. *Nanotechnology* **2008**, *19*, 215714.
(11) Izaki, M.; Omi, T. *Appl. Phys. Lett.* **1996**, *68*, 2439.
(12) Peulon, S.; Lincot, D. *J. Electrochem. Soc.* **1998**, *145*, 864.
(13) Pauporté, T.; Lincot, D. *Appl. Phys. Lett.* **1999**, *75*, 3817.
(14) Pauporté, T.; Lincot, D. *Electrochim. Acta* **2000**, *45*, 3345.
(15) Liu, R.; Vertegel, A. A.; Bohannan, E. W.; Sorenson, T. A.; Switzer, J. A. *Chem. Mater.* **2001**, *13*, 508.
(16) Pauporté, T.; Cortès, R.; Froment, M.; Beaumont, B.; Lincot, D. *Chem. Mater.* **2002**, *14*, 4702.
(17) Yoshida, T.; Komatsu, D.; Shimokawa, N.; Minoura, H. *Thin solid films* **2004**, *451*, 166.
(18) Könenkamp, R.; Word, R. W.; Schlegel, C. *Appl. Phys. Lett.* **2004**, *85*, 6004.
(19) Könenkamp, R.; Word, R. W.; Godinez, M. *Nano Lett.* **2005**, *5*, 2005.
(20) Tena-Zaera, R.; Elias, J.; Wang, G.; Lévy-Clément, C. *J. Phys. Chem. C* **2007**, *111*, 16706.
(21) Cui, J. B.; Soo, Y. C.; Chen, T. P.; Gibson, U. J. J. *Phys. Chem. C* **2008**, *112*, 4475.
(22) Nadarajah, A.; Word, R. C.; Meiss, J.; Könenkamp, R. *Nano Lett.* **2008**, *8*, 534.
(23) Pauporté, T.; Lincot, D. *J. Electroanal. Chem.* **2001**, *517*, 54.
(24) Goux, A.; Pauporté, T.; Lincot, D. *Electrochim. Acta* **2006**, *51*, 3168.
(25) Chen, J.; Aé, L.; Aichele, C.; Lux-Steiner, M. *Appl. Phys. Lett.* **2008**, *92*, 161906.
(26) Pauporté, T.; Lincot, D.; Viana, B.; Pellé, F. *Appl. Phys. Lett.* **2006**, *89*, 233112.
(27) Donderis, V.; Hermandez-Fenollosa, M. A.; Damonte, L. C.; Mari, B.; Cembrero, J. *Superlattices Microstruct.* **2007**, *42*, 461.
(28) Pauporté, T.; Lincot, D. *Adv. Mater. Opt. Electron.* **1995**, *5*, 289.
(29) Goux, A.; Pauporté, T.; Chivot, J.; Lincot, D. *Electrochim. Acta* **2005**, *50*, 2239.
(30) Rousset, J.; Saucedo, E.; Lincot, D. *Chem. Mater.* **2009**, *21*, 534.
(31) Burstein, E. *Phys. Rev.* **1954**, *93*, 632.
(32) Moss, T. S. *Proc. Phys. Soc. London* **1964**, *B67*, 775.
(33) Roth, A. P.; Webb, J. B.; Williams, D. F. *Solid State Commun.* **1981**, *39*, 1269.
(34) Tam, K. H.; Cheung, C. K.; Leung, Y. H.; Djurii, A. B.; Ling, C. C.; Beling, C. D.; Fung, S.; Kwok, W. M.; Chan, W. K.; Phillips, D. L.; Ding, L.; Ge, W. K. *J. Phys. Chem. B* **2006**, *110*, 20865.
(35) Tena-Zaera, R.; Elias, J.; Lévy-Clément, C.; Bekeny, C.; Voss, T.; Mora-Sero, I.; Bisquert, J. *J. Phys. Chem. C* **2008**, *112*, 16318.
(36) Hahn, B.; Heindel, G.; Pschorr-Schoberer, E.; Gebhardt, W. *Semicond. Sci. Technol.* **1998**, *13*, 788.
(37) Tchelidze, T.; Chikoidze, E.; Gorochov, O.; Galtier, P. *Thin Solid Films* **2007**, *515*, 8744.
(38) Chikoidze, E.; Nolan, M.; Modreanu, M.; Sallet, V.; Galtier, P. *Thin solid Films* **2008**, *516*, 8146.
(39) Tao, Z.; Yu, X.; Fei, X.; Liu, J.; Yang, G.; Zhao, Y.; Yang, S.; Yang, L. *Optical Mater.* **2008**, *31*, 1.
(40) Pauporté, T. et al., to be published.
(41) Park, W. I.; Yi, G. C. *Adv. Mater.* **2004**, *16*, 87.
(42) Dittrich, T.; Kieven, D.; Rusu, M.; Belaidi, A.; Tornow, J.; Schwarzburg, K. *Lux-Steiner M. Appl. Phys. Lett.* **2008**, *93*, 053113.
(43) Law, M.; Greene, L. E.; Johnson, J. C.; Saykally, R.; Yang, R. *Nat. Mater.* **2005**, *4*, 455.
(44) Tien, L. C.; Sadik, P. W.; Norton, D. P.; Voss, L. F.; Pearton, S. J.; Wang, H. T.; Kang, B.; et al. *Appl. Phys. Lett.* **2005**, *87*, 222216.
(45) Tseng, Y. K.; Huang, C. J.; Cheng, H. M.; Lin, I. N.; Liu, K. S.; Chen, I. C. *Adv. Funct. Mater.* **2003**, *13*, 811.
(46) Li, S. Y.; Lin, P.; Lee, C. Y.; Tseng, T. Y. *J. Appl. Phys.* **2004**, *95*, 3711.
(47) Wang, Z.; Song, J. *Science* **2006**, *312*, 242.
(48) Badre, C.; Pauporté, T.; Turmine, M.; Lincot, D. *Nanotechnology* **2007**, *18*, 365705.
(49) Okada, T.; Kawashima, K.; Ueda, M. *Appl. Phys. A: Mater. Sci. Process.* **2005**, *81*, 907.
(50) Cui, J. *J. Phys. Chem. C* **2008**, *112*, 10385.
(51) Varshni, Y. P. *Physica* **1967**, *34*, 149.

JP9010179